

Exploring Multi-layer Graphene Nanoribbon Interconnects

Sansiri Tanachutiwat and Wei Wang

College of Nanoscale Science and Engineering,
State University of New York at Albany, 255 Fuller Rd., Albany, NY, USA
`{stanachutiwat,wwang}@uamail.albany.edu`

Abstract. In this paper, an improvement of the existing conductance model for the single-layer GNR and a novel conductance model for multi-layer GNR are introduced. The models leverage the recent theoretical and theoretical results, providing consistent conductance/resistance estimations with the experimental results. Using these models, comparison of the resistance of multi-layer GNR with Cu and CNT bundle for the same aspect ratio is carried out. The results demonstrate that multi-layer GNR will be a superior interconnect solution over Cu for 45nm or less technology nodes. This work introduced a promising graphene interconnect by utilizing multiple layers. This might lead to future breakthrough of the new emerging interconnect solution.

Keywords: Graphene, Interconnect, Conductance, Modeling.

1 Introduction

Graphene nanoribbon (GNR) is essentially a monolayer of graphite patterned into a narrow strip, which expected to share many fascinating electrical, mechanical and thermal properties with graphene and carbon nanotube (CNT). Similar to CNT, GNR has a ballistic transport for a very long MFP (in micrometer range) and conduct a large current density in the same order of magnitude reported by CNT [1-5]. The main advantage of GNR over CNT is the lithographic pattern-ability. The chirality of CNT is random during fabrication and the conventional planar process can not be used. But GNR can be fabricated using lithographic pattern technology and its chirality can be tuned by the orientation of the edge termination. Thus, metallic and semiconducting GNR can be controlled to build interconnects and devices respectively, which offers the promise of a large integration of graphene-based interconnects and devices to build future integrated circuits.

In order to provide an efficient on-chip interconnect solution, the multi-layer GNR needs to be considered, which might potentially lower the overall resistance. The stack of GNR layers can be formed during almost all growth processes. Each layer will have around 0.34nm distance due to van de Waal effect.

In this paper, we analyzed the performance of such multi-layer GNRs considering chirality, width, Fermi level shift and effect of electron scattering at the edges. Our

results show that multi-layer GNRs can outperform copper and carbon nanotube in terms of resistance, leading to a promising interconnect solution.

2 Conductance Modeling of Multi-layer GNR

2.1 Single-Layer GNR Conductance

The conductance of a GNR layer depends on the number of the quantum channels and the electron mean free path. It can be calculated as [8]:

$$G = \frac{G_Q \lambda}{L} , \quad (1)$$

where G_Q , λ and L are the quantum conductance of graphene ($G_Q = 4e^2/h$ [5,8-9]), the electron mean free path (MFP) considering N_{ch} quantum channels and the length of the GNR, respectively. Since G_Q is a constant and L is a predefined value, we can calculate the conductance G by determining the values of N_{ch} and λ . The calculation of these two values can be found in [6], which are based on: 1) effect of electron scattering, 2) width confinement, 3) GNR chirality, and 4) Fermi level shift. However, the intrinsic and extrinsic phonon scattering effects are not included. Recent results demonstrated that these two phonon effects have a significant impact on λ [10-12].

The results in [5,11] demonstrated that the scattering of intrinsic acoustic phonons (AP) and extrinsic remote interfacial phonons (RIP) due to SiC or SiO₂ substrates will reduce λ . Based on these results, we have:

$$\lambda^{-1} = \lambda_e^{-1} + \lambda_{AP}^{-1} + \lambda_{RIP}^{-1} . \quad (2)$$

where λ_e , λ_{AP} and λ_{RIP} denote MFP due to electron, intrinsic AP, and extrinsic RIP scattering, respectively. The calculation of λ_e is based on the method in [6] with the modification of N_{ch} to include the subbands above Fermi level within a few kT [8].

Electron scattering consists of scattering in the longitudinal direction due to defects λ_{defect} (the first subbands) as well as scattering in the transverse direction due to edge effect (higher subbands). The effect of width confinement is considered in the estimation of $\Delta E = h\nu_F/2W$ [6]. The effect of GNR chirality will decide the GNR to be metallic or semiconducting. The metallic GNR has the conduction of the first subband, while the semiconducting GNR does not have the subband, leading to a smaller conductance value [6]. Therefore, the electron scattering MFP is:

$$\lambda_e = \lambda_{\text{defect}} + W \sum_{n=1}^{N_{ch}} \sqrt{\left(\frac{N_{ch}}{n}\right)^2 - 1} . \quad (3)$$

The effect of Fermi level shift is due to the charge accumulated at the surface between GNR and substrate/dielectric. This E_F shift from the Dirac point will lead to

more conduction channels N_{ch} . The MFP values due to the two phone scattering effects, AP scattering λ_{AP} and RIP scattering λ_{RIP} , can be calculated based on the results in [11-12] as:

$$\lambda_{AP} = \frac{h^2 \rho_s v_s^2 v_F^2 l}{\pi^2 D_A^2 k_B T} \text{ and } \lambda_{RIP} = \alpha l V_g^{1.02} \left(e^{E_0/kT} - 1 \right), \quad (4)$$

where $v_F = 10^6$ m/s is the Fermi velocity, $v_s = 2.1 \times 10^4$ m/s is the sound velocity, $D_A = 17 \pm 1$ eV [11] is the acoustic deformation potential, and $\rho_s = 6.5 \times 10^{-7}$ kg/m² [11] is the 2D mass density of graphene. For SiO₂ substrate, $\alpha = 0.306$ V^{-1.02} and $E_0 = 104$ meV are obtained from experimental results [11-12]. For the SiC substrate, these parameters will be different and can be found in [12]. Note that both λ_{AP} and λ_{RIP} are temperature dependant. Also, since $\lambda_{RIP} \ll \lambda_{AP}$, the effect of RIP is more significant than that of AP.

By using (2)-(4), we can estimate the conductance of various single-layer GNRs. The estimation results based on the proposed model are more consistent with the measured results of [1, 4] than the results using [6], demonstrating the efficiency of the proposed method.

2.2 Multi-layer GNR Conductance

Based on the above conductance model of the single-layer GNR, we now derive the conductance model of the multi-layer GNR. The number of GNR layer can be considered as $M = \lfloor AR \cdot W / \delta \rfloor$, where AR is the aspect ratio of the interconnects defined in [13] and $\delta \approx 0.34$ nm is the inter-layer distance. We have $i = 1, 2, \dots, M$ to identify each layer in an M -layer GNR.

The effect of charges accumulated at the substrate surface will cause the Fermi level shift. This effective Fermi level shift is observed to decrease exponentially as the layer is away from the substrate, and becomes negligible after the fifth layer [5]. Therefore, for the i^{th} layer and $i \leq 4$, the Fermi level E_F will decay by $e^{-\delta i/\beta}$, where $\beta = 0.387$ nm obtained from the fitting curve in [5]. This decay factor is similar to the screening length effect of metal materials reported in [14]. Besides the Fermi level shift, the RIP scattering will disappear when the layer is away from the substrate/dielectric. This effect has been experimentally observed such that it can be neglected after the second layer [11].

Based on the above analysis, we can get G_i for each layer by using $E_{F,i}$ in (3)-(4). Then, we obtain the total conductance of an M -layer GNR as:

$$G_{GNR} = \sum_{i=1}^M G_i, \quad (5)$$

In order to demonstrate the efficiency of the proposed model (5), we estimate the conductance of a 6-layer GNR [5]. The simulation result matches the experiment result.

3 Conductance Comparison

Using the proposed multi-layer GNR conductance models, we estimate the conductance of various GNR interconnect solutions and compare the results with copper [13], monolayer SWCNT and mixed CNT bundle [8] as shown in Fig. 1. It is seen in Fig. 1 that the single-layer GNR has a higher resistance than CNT and Cu wires, which is consistent with the result in [8]. But for the same aspect ratio, the metallic multi-layer GNR has a lower resistance than Cu and the CNT bundle. For the 45nm, 32nm, 22nm and 16nm technology nodes, the improvements of the multi-layer GNR over Cu are 12.8%, 46.1%, 68.8% and 81.4%, respectively. Note that the semiconducting GNR will have a poor conductance performance, which is consistent with the measurement results in [3]. Therefore, in order to utilize the multi-layer GNR, more metallic layers are required to provide an efficient interconnect solution.

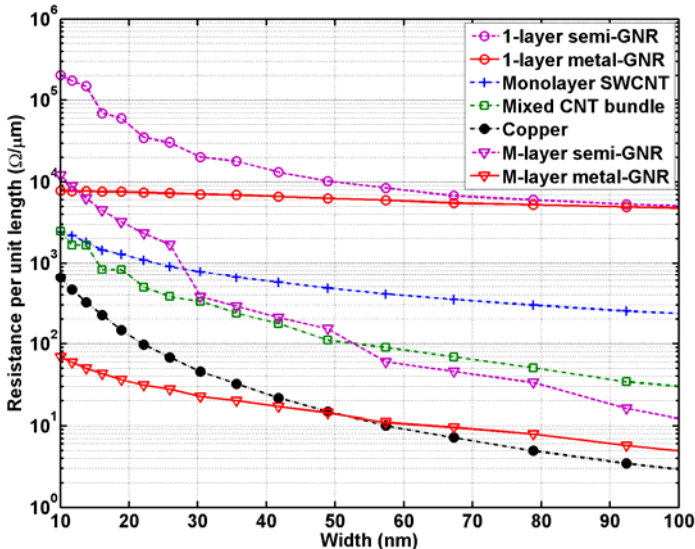


Fig. 1. Comparison of resistance per unit length versus different width of different technology nodes for various interconnect materials. i.e. single-layer GNR obtained from [6], the proposed single-layer GNR, proposed multi-layer GNR (aspect ratios are obtained from [13]), carbon nanotube bundle 8 (aspect ratios are obtained from [13]), single-layer carbon nanotube array [8] and copper interconnect [13].

4 Conclusion

In this paper, we improved the existing conductance models for the single-layer GNR and introduced a novel conductance model for multi-layer GNR. The models leverage the recent theoretical and theoretical results, providing a consistent conductance/resistance estimation with the experimental results. Using these models, we compared the conductance of multi-layer GNR with Cu for the same aspect ratio. The results

demonstrate that multi-layer GNR will be a superior interconnect solution over Cu for 45nm or less technology nodes.

The novelty of this work is that the new conductance model of GNR considers the realistic substrate/dielectric and layer effect. The results leading to a promising multi-layer graphene interconnect solution. The significance is that the introduction the multi-layer GNR interconnect concepts and models might lead to future breakthrough of the new emerging interconnect solution.

Acknowledgment

This work has been supported in part by the AFSTTR and MARCO (via IFC Center). Useful discussions with Ji Ung Lee and Robert Geer are gratefully acknowledged.

References

1. Berger, C., et al.: Electronic Confinement and Coherence in Patterned Epitaxial Graphene. *Science* 312(5777), 1191–1196 (2006)
2. Hass, J., et al.: Why Multilayer Graphene on 4H-SiC(0001) Behaves Like a Single Sheet of Graphene. *Phys. Rev. Lett.* 100, 125504 (2008)
3. Han, M.Y., Zyilmaz, B.O., Zhang, Y., Kim, P.: Energy Band-Gap Engineering of Graphene Nanoribbons. *Phys. Rev. Lett.* 98, 206805 (2007)
4. Chen, Z., Lin, Y., Rooks, M.J., Avouris, P.: Graphene nano-ribbon electronics. *Physica E* 40(2), 228–232 (2007)
5. Wang, H.M., Wu, Y.H., Ni, Z.H., Shen, Z.X.: Electronic transport and layer engineering in multilayer graphene structures. *Applied Physics Letters* 92, 03504 (2008)
6. Naeemi, Meindl, J.D.: Conductance Modeling for Graphene Nanoribbon (GNR) Interconnects. *IEEE Electron Device Letters* 28(5), 428–431 (2007)
7. Cserti, J., Csordás, A., Dávid, G.: Role of the Trigonal Warping on the Minimal Conductivity of Bilayer Graphene. *Phys. Rev. Lett.* 99, 066802 (2007)
8. Haruehanroengra, S., Wang, W.: Analyzing Conductance of Mixed Carbon-Nanotube Bundles for Interconnect Applications. *IEEE EDL* 28(8), 756–759 (2007)
9. Latil, S., Henrard, L.: Charge Carriers in Few-Layer Graphene Films. *Phys. Rev. Lett.* 97(3), 036803 (2006)
10. Jang, S.A., Chen, J.H., Williams, E.D., Sarma, S.D., Fuhrer, M.S.: Tuning the Effective Fine Structure Constant in Graphene: Opposing Effects of Dielectric Screening on Short- and Long-Range Potential Scattering. <http://arxiv.org/abs/0805.3780v1>
11. Chen, J.H., Jang, C., Xiao, S., Ishigami, M., Fuhrer, M.S.: Intrinsic and Extrinsic Performance Limits of Graphene Devices on SiO₂. *Nature Nanotech*, 206–209 (2008)
12. Fratini, S., Guinea, F.: Substrate-Limited Electron Dynamics in Graphene. *Phys. Rev. B* 77, 195415 (2008)
13. International Technology Roadmap for Semiconductor (ITRS 2007) (2007), <http://public.itrs.net>
14. Ohta, T., et al.: Interlayer Interaction and Electronic Screening in Multilayer Graphene Investigated with Angle-Resolved Photoemission Spectroscopy. *Phys. Rev. Lett.* 98, 206802 (2007)